

On the interaction of solar near-relativistic electrons with back-scatter regions beyond 1 AU

N. Agueda^{1*}, R. Vainio^{*}, D. Lario[†] and B. Sanahuja^{2**}

^{*}*Department of Physics, University of Helsinki, 00014 Helsinki, Finland*

[†]*Applied Physics Laboratory, The Johns Hopkins University, Laurel, MD 20723-6099, USA*

^{**}*Departament d'Astronomia i Meteorologia, Universitat de Barcelona, 08028 Barcelona, Spain*

Abstract. We study the near-relativistic (NR; >30 keV) electron event observed on 2000 February 18 by the *Advanced Composition Explorer* spacecraft. Highly collimated pitch-angle distributions were observed during the first ~ 2 h of the event. Roelof (2008) explained this event by assuming that the propagation of NR electrons is essentially "scatter-free" in the inner heliosphere and that beyond 1 AU, particles are "back-scattered" by magnetic field compressions and irregularities. We use Monte Carlo simulations to explore this approach. We fit observational sectorized intensities to assure that the directional information contained in the data is used in full. We conclude that the event cannot be explained without assuming a back-scatter region beyond 1 AU and that NR electrons propagated under weak-scattering conditions in the inner heliosphere.

Keywords: Energetic particles, Interplanetary propagation, Particle acceleration

PACS: 96.50.Vg, 96.50.sh, 96.50.Pw

INTRODUCTION

Pitch-angle distributions (PADs) of near-relativistic (NR; >30 keV) electrons that are highly collimated along the interplanetary magnetic field (IMF) during the rise-to-maximum phase of solar energetic particle (SEP) events have been interpreted as evidence that the NR electron propagation in the inner heliosphere can be (at least in some regions and under some circumstances) nearly "scatter-free" [1, 2, 3].

In this paper we study the NR electron event observed by the *Advanced Composition Explorer* (ACE), which showed highly collimated PADs at its onset [2, 3]. A previous work [4] assumed that during this event NR electrons propagated "scatter-free" along the IMF lines connecting the source region at the corona with the observer but further out particles were "back-scattered" inward from beyond 1 AU by magnetic field compressions and irregularities [4]. In this approach the propagation is assumed not to be scatter-free beyond 1 AU. This approximation allows the inference of the injection history of the first-crossing solar electrons directly from the data without any propagation modeling by utilizing unidirectional intensities from two preferred directions (sunward and anti-sunward) and assuming that the in-going particles undergo mirroring and conserve their magnetic moment.

Our goal is to re-examine the 2000 February 18 electron event, as observed by the LEFS60 telescope of the EPAM experiment on ACE [5], using observational sectorized intensities. We use a Monte Carlo transport model to simulate the propagation of SEPs along the interplanetary magnetic field [6, 7]. This allows us to explore different propagation scenarios and to test the assumptions made in studies like [4].

In Section 2 we review the transport model and the fitting technique. Section 3 gives an overview of the results of deconvolving the directional intensities observed during the NR electron event. Section 5 summarizes the results.

THE MODEL

Interplanetary transport

We use a Monte Carlo model to simulate the interplanetary transport of SEPs injected at the root of an Archimedean spiral magnetic field line. The transport processes included are the following: particle streaming along the magnetic field lines, pitch-angle focusing by the diverging IMF, pitch-angle scattering by magnetic field fluctuations, adiabatic deceleration resulting from the interplay of scattering and focusing and solar wind convection [8, 9]. The results of the simulation give the directional distribution of particles at 1 AU, as a function of time and the energy range of interest (see [6] for details).

As initial condition we consider all particles to be injected instantaneously at two solar radii from the center

¹ Now at the Space Sciences Laboratory, University of California, Berkeley, CA 94720, USA

² Also at the Institut de Ciències del Cosmos, Universitat de Barcelona, 08028 Barcelona, Spain

of the Sun. Thus, the results of the simulation are expressed in terms of Green's functions of particle transport. The energy spectrum of the solar source is described by a power law ($dN/dE \propto E^{-\gamma_s}$) with spectral index γ_s , which is estimated from the observational data.

In the solar wind frame, the pitch-angle diffusion coefficient can be expressed as $D_{\mu\mu} = v(1 - \mu^2)/2$, where v is the scattering frequency and μ is the particle pitch-angle cosine. We assume $v(\mu) = v_0 \left(\frac{|\mu|}{1+|\mu|} + \varepsilon \right)$, where ε allows us to simulate different scattering conditions, from quasi-isotropic ($\varepsilon \geq 1$) to fully anisotropic ($\varepsilon = 0$, totally decoupled hemispheres in the μ -space). The scattering rate, v_0 , is determined from the mean free path parallel to the field $\lambda_{||}$, or the radial mean free path λ_r , which are related by

$$\frac{\lambda_r}{\cos^2 \psi} = \lambda_{||} = \frac{3v}{4} \int_{-1}^{+1} \frac{1 - \mu^2}{v(\mu)} d\mu \quad (1)$$

where v is the particle speed and ψ is the angle between the magnetic field and the radial direction [10]. We assume that the radial mean free path is constant, independent of the radial distance and energy, as proposed by previous works [11, 12]. Particle transport perpendicular to the magnetic field is neglected.

We adapt the model to be able to differentiate two different transport regimes in the inner and outer heliosphere. We assume that in the inner heliosphere $\lambda_r = \lambda_1$. The back-scatter region is assumed to be located at $r \geq r_{bs}$ (where $r_{bs} > 1$ AU); in this region we assume isotropic scattering ($v(\mu) = v_0$) and $\lambda_r = \lambda_2$. We vary r_{bs} from 1.1 AU to 1.6 AU with steps of 0.1 AU and we also consider the case $r_{bs} = \infty$.

Fitting sectored intensities

The goal is to solve the inversion problem of inferring the transport parameters (i.e. λ_1 , λ_2 and r_{bs}) and the injection time profile at the Sun from a set of in-situ measured sectored intensities $I^s(t)$, where $I^s(t)$ is the intensity measured at time t by sector s in a given energy channel. By taking into account the angular response of the sectors scanned by the LEFS60 telescope, we are able to transform the simulated pitch-angle distributions into sectored intensities measured by the telescope [6]. The modeled sectored intensities, $M^s(t; \lambda_1, \lambda_2, r_{bs})$, in sector s can be written as

$$M^s(t; \lambda_1, \lambda_2, r_{bs}) = \int_{T_1}^{T_2} dt' g^s(t, t'; \lambda_1, \lambda_2, r_{bs}) q(t'), \quad (2)$$

where $q(t)$ -to be determined- represents the electron injection function and $g^s(t, t'; \lambda_1, \lambda_2, r_{bs})$ represents the contribution of an impulsive injection to the modeled

intensities for a given sector s , at a given time t , when the injection of NR electrons took place at time t' .

By taking into account the number of sectors of the telescope and discrete values of time, we determine the best-fit injection function by comparing the modeled intensities with the observations. Let b be the pre-event averaged background intensity and $J_i = I_i - b$, where $i = 1, 2, \dots, n$ numbers the observational points. We want to derive the m -vector \vec{q} that minimizes the length of the n -vector $\vec{J} - \vec{M}$, that means minimizing the value of $\|\vec{J} - \vec{M}\| \equiv \|\vec{J} - \mathbf{g} \cdot \vec{q}\|$, subject to the constraint that $q_j \geq 0 \forall j = 1, 2, \dots, m$, where j indexes the injection times. The best-fit injection function is taken to be a combination of m delta-function injection amplitudes at times t_j . To solve this inversion problem and obtain the best-fit injection values, we use a non-negative least squares method [13].

The best-fit transport parameters (λ_1 , λ_2 and r_{bs}) are determined by minimizing a goodness-of-fit estimator $\zeta = \sum_i (\log J_i - \log M_i)^2$, which computes the sum of the squared logarithmic differences between the observational J_i and the modeled M_i sectored intensities in each energy channel. The calculation of the goodness of the fit is restricted to the time interval selected for the simulation. The goodness-of-fit estimator of the whole fit is obtained by adding the values obtained for each energy channel.

RESULTS

We use electron intensities measured by the LEFS60 detector (60° to the spacecraft spin axis) of the EPAM experiment on board *ACE* in three energy ranges: E'2 (62–102 keV), E'3 (102–175 keV) and E'4 (175–312 keV) [5]. The LEFS60 telescope utilizes the spin of the spacecraft to define eight sectors [5], such that particle anisotropy can be studied by comparing counting rates from each sector.

We study the NR electron event observed on 2000 February 18 by LEFS60 from 09:30 UT to 11:15 UT. During this period, there was a data gap in the coverage of the solar wind experiment on *ACE*. The solar wind speed observed by the *Wind* spacecraft ranged from 370 to 390 km s⁻¹. Thus, for the modeling of the event, we assume that the spacecraft was embedded in a 350 km s⁻¹ solar wind stream. The IMF vector at *ACE* was very stable and each sector scanned roughly the same pitch-angle cosine range. The pitch-angle cosine range scanned by the LEFS60 telescope was high ($\sim 82\%$) [14].

The first NR electrons were detected above the pre-event background at 09:32 UT in the E'4 channel. During the event, highly collimated PADs were observed [2, 3, 15], e.g. the peak intensity observed in the sector scanning particles propagating from the Sun along

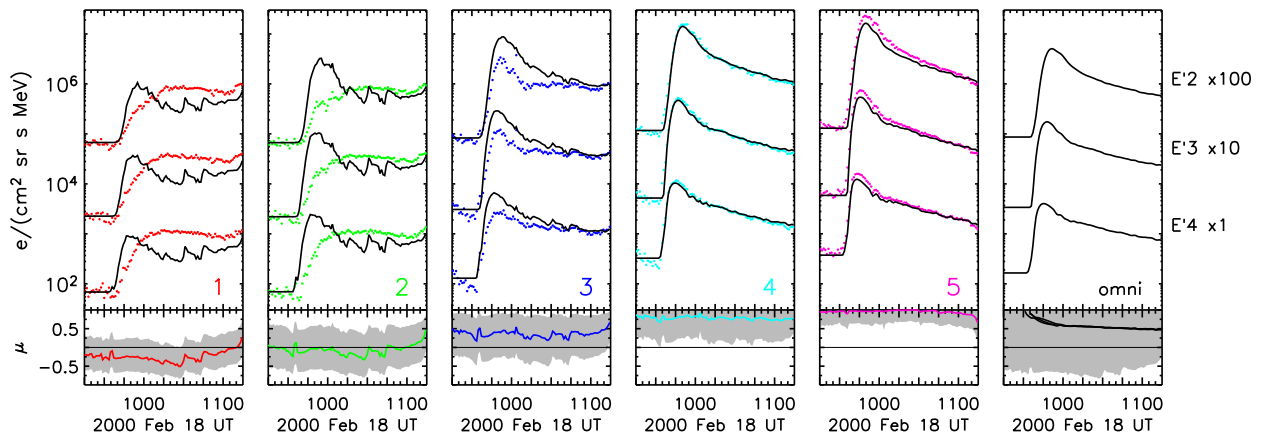


FIGURE 1. NR electron event on 2000 February 18 as observed by five of the sectors of the LEFS60 telescope in three energy channels: E'4 175-312 keV, E'3 102-175 keV (x10), and E'2 62-102 keV (x100). Sectors are labeled from 1 to 5; due to the stability of the interplanetary magnetic field, they provide all the directional information contained in the data. The dots show the observational data and the curves show the modeled sectorized intensities for scenario A. The lower panels show the pitch-angle cosine of the midpoint clock-angle zenith direction of the sector (curve) and the scanned pitch-angle cosine range (gray area) as a function of time. The last graph shows the omnidirectional intensities and the mean pitch-angle cosine deduced from the simulation with the gray area showing the pitch-angle cosine range scanned by the telescope.

the IMF direction was more than one order of magnitude higher than the peak intensity measured by the sector which mainly scanned electrons propagating sunward (see Figure 1 in [3]). The maximum intensity was observed at 09:45/09:47/09:52 UT in the E'4/E'3/E'2 energy channels, respectively. The spectral index of the maximum spin-averaged differential intensities was $\gamma_{\max} = 2.2$. We can estimate an upper limit of the spectral index of the source, γ_s , if we assume that the mean free path is independent of the energy and that the effects of adiabatic deceleration on NR electrons are negligible. If we assume $v \propto E^{1/2}$ for non-relativistic particles, then $\gamma_s = \gamma_{\max} + 0.5 = 2.7$.

The NR electron event was associated with a C1.1 X-ray solar flare from approximately S16 W78 in the NOAA active region 8867 [16]. The 1-8 Å X-ray emission lasted from 09:21 to 09:38 UT, peaking at 09:27 UT. A type III radio burst was observed at 09:24 UT at 14 MHz [17] by the WAVES experiment on the *Wind* spacecraft [18]. The solar radio event included a series of type II radio bursts, first seen at 70 MHz around 09:24 UT, and lasting for more than 20 minutes [16]. A CME was also associated with this event, first seen by LASCO/C2 at 09:54 UT at $4.15R_{\odot}$, and propagating at 890 km s^{-1} according to the *SOHO/LASCO* CME Catalog [19]³.

We simulate the event by considering two different propagation scenarios. In Scenario A we assume that there is no back-scatter region (i.e. it can be considered to

TABLE 1. Best fit parameters for different transport scenarios (see text for details)

Scenario	Inner heliosphere		Back-scatter region	ζ
	λ_1 (AU)	r_{bs} (AU)		
A	1.1	no back-scatter region		152
B	scatter-free	1.1	0.02	303

be very distant from the observer $r_{bs} \rightarrow \infty$), the scattering is μ -dependent with $\varepsilon = 0.01$ and $\lambda_1 \in [0.5, 1.5]$ AU. In scenario B we assume scatter-free propagation in the inner heliosphere ($\lambda_1 \rightarrow \infty$) and $\lambda_2 \in [0.01, 0.5]$ AU with the back-scatter region at $r_{bs} \in [1.1, 1.6]$ AU.

The best-fit transport parameters for each scenario are listed in Table 1. The NR electron event cannot be explained assuming an Archimedean IMF and no back-scatter region beyond 1 AU (scenario A) because the intensities measured by those sectors that scan particles propagating sunward cannot be satisfactorily reproduced (see Figure 1). If we assume scatter-free propagation in the inner heliosphere and a back-scatter region beyond 1.1 AU with $\lambda_2 = 0.02$ AU (scenario B), the fit succeeds in better reproducing the observed sunward intensities (see Figure 2). However scenario B cannot explain the intensities observed by those sectors scanning mainly particles with $0 \leq \mu < 1$, because the PADs predicted by the model at 1 AU are too collimated along the IMF vector. This result suggests that the propagation of NR electrons in the inner heliosphere was not purely scatter-free but they suffered weak pitch-angle scattering.

³ http://cdaw.gsfc.nasa.gov/CME_list/

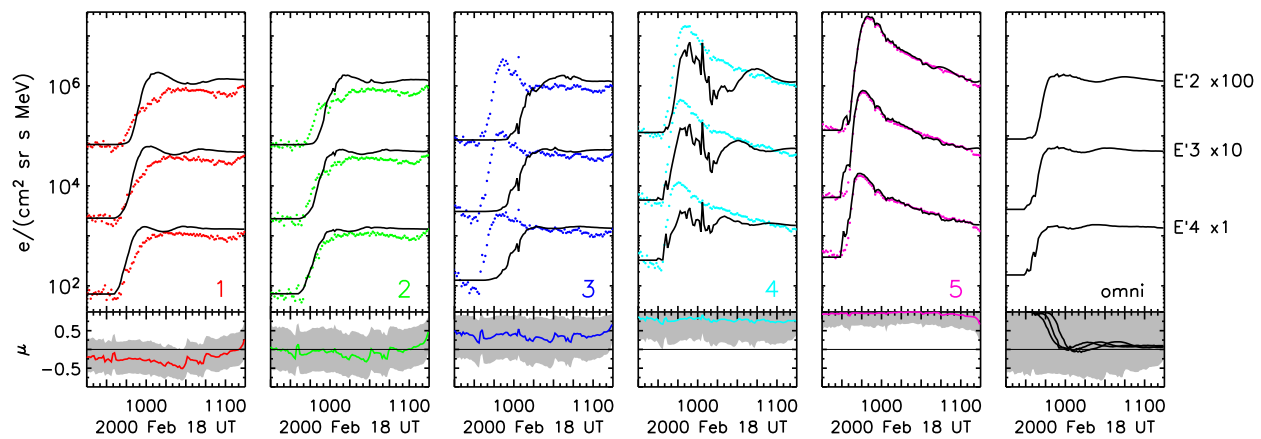


FIGURE 2. Same as in Figure 1 for scenario B

The best-fit injection profile inferred for scenario B begins at $\sim 09:20$ UT and lasts at least 1.5 hours, peaking at 09:31 UT, that is a 4 min delay between the beginning of the injection and the timing of the metric and decametric radio bursts, which started at the Sun at 09:16 UT. If the observed CME propagated radially with a constant speed of 890 km s^{-1} , it would have been located at $\sim 2R_{\odot}$ at the beginning of the electron injection.

We believe that more simulations are needed to correctly reproduce the observed sectorized intensities and obtain more information about the scattering conditions in the inner heliosphere. This would allow us to obtain a better estimation of the electron injection profile, revisit the delays between the electron injection and the observed radio bursts and CME, and thus provide more information about the solar source injecting NR electrons into interplanetary space during this event.

SUMMARY AND CONCLUSIONS

We have investigated the hypothesis that the propagation of NR electrons can be, in some cases, essentially "scatter-free" in the inner heliosphere and that beyond 1 AU, particles can be "back-scattered" by magnetic field compressions and irregularities. We have used a Monte Carlo transport model to explore this approach by simulating two transport regimes along an Archimedean IMF: (1) a large radial mean free path ($\lambda_r > 0.5$ AU) and anisotropic scattering in the inner heliosphere, and (2) a small radial mean free path ($\lambda_r < 0.5$ AU) and isotropic scattering in the back-scatter region.

We have applied the model to the 2000 February 18 electron event observed by the ACE spacecraft. We find that the PADs observed during this event cannot be explained without assuming a back-scatter region beyond 1 AU.

ACKNOWLEDGMENTS

NA and RV acknowledge the financial support of the Academy of Finland (110021, 121650, and 124837). BS is grateful for the financial support of the Spanish Ministerio de Ciencia y Tecnología (AYA2007-60724). DL was partially supported by NSF (ATM-0648181) and NASA (NNX09AG30G). NA acknowledges the Magnus Ehrnrooth Foundation for sponsoring her participation in the 12th International Solar Wind Conference.

REFERENCES

1. S. Krucker et al., *Astrophys. J.*, **519**, 864 (1999).
2. D.K. Haggerty and E.C. Roelof, *Astrophys. J.*, **579**, 841 (2002).
3. G.M. Simnett, E.C. Roelof, and D.K. Haggerty, *Astrophys. J.*, **579**, 854, (2002).
4. E.C. Roelof, *AIP Conf. Proceedings*, **1039**, 174 (2008).
5. R.E. Gold et al., *Space Science Rev.*, **86**, 541, (1998).
6. N. Agueda et al., *Astrophys. J.*, **675**, 1601, (2008).
7. N. Agueda et al., *Astron. Astrophys.*, *accepted* (2009).
8. L. Kocharov et al., *Solar Phys.*, **182**, 195, (1998).
9. R. Vainio, L. Kocharov, and T. Laitinen, *Astrophys. J.*, **528**, 1015, (2000).
10. K. Hasselmann, and G. Wibberenz, *Z. Geophys.*, **34**, 353, (1968).
11. M.B. Kallenrode, G. Wibberenz, and S. Hucke, *Astrophys. J.*, **394**, 351, (1992).
12. W. Dröge, *Astrophys. J.*, **589**, 1027, (2003).
13. C.L. Lawson, and R.J. Hanson, *Solving Least Squares Problems* (Englewood Cliffs: Prentice-Hall), (1974).
14. N. Agueda et al., *Adv. Space Res.*, **44**, 794, (2009).
15. W. Dröge, and Y.Y. Kartavykh, *Astrophys. J.*, **639**, 69, (2009).
16. D.J.F. Maia, and M. Pick, *Astrophys. J.*, **609**, 1082, (2004).
17. H.V. Cane, W.C. Erickson, and N.P. Prestage, *J. Geophys. Res.*, **107**, 1315, (2002).
18. J.L. Bougeret et al., *Space Science Rev.*, **71**, 231, (1995).
19. S. Yashiro et al., *J. Geophys. Res.*, **109**, 7105, (2004).